Impact of diatom-diazotroph associations on carbon export in the Amazon River plume

Laurence Y. Yeung,[1] William M. Berelson,[2] Edward D. Young,[1] Maria G. Prokopenko,[2] Nick Rollins,[2] Victoria J. Coles,[3] Joseph P. Montoya,[4] Edward J. Carpenter,[5] Deborah K. Steinberg,[6] Rachel A. Foster,[7] Douglas G. Capone,[8] and Patricia L. Yager[9]

Received 1 August 2012; accepted 10 August 2012; published 25 September 2012.

[1] Offshore tropical river plumes are associated with areas of high N_2 fixation (diazotrophy) and biological carbon drawdown. Episodic blooms of the diatom *Hemiaulus hauckii* and its diazotrophic cyanobacterial symbiont *Richelia intracellularis* are believed to dominate that carbon drawdown, but the mechanism is not well understood. We report primary productivity associated with blooms of these diatom-diazotroph assemblages (DDAs) in the offshore plume of the Amazon River using simultaneous measurements of O_2/Ar ratios and the triple-isotope composition of dissolved O_2. In these blooms, we observe peaks in net community productivity, but relatively small changes in gross primary productivity, suggesting that DDA blooms increase the ecosystem carbon export ratio more than twofold. These events of enhanced export efficiency lead to biological uptake of dissolved inorganic carbon and silicate, whose longer mixed-layer residence times otherwise obscure the differential impact of DDAs. The shorter-term rate estimates presented here are consistent with the results derived from longer-term geochemical tracers, confirming that DDAs drive a significant biological CO_2 pump in tropical oceans. **Citation:** Yeung, L. Y., et al. (2012), Impact of diatom-diazotroph associations on carbon export in the Amazon River plume, *Geophys. Res. Lett.*, *39*, L18609, doi:10.1029/2012GL053356.

1. Introduction

[2] The freshwater outflow of the Amazon River reaches thousands of kilometers from the river mouth, influencing biogeochemistry in the otherwise nutrient-starved western tropical North Atlantic (WTNA). The resulting surface plume is characterized by a significant undersaturation in CO_2 and dissolved inorganic carbon (DIC) linked to new production [*Ternon et al.*, 2000; *Körtzinger*, 2003; *Cooley and Yager*, 2006]. Previous estimates of net production in the seasonal Amazon plume suggest that up to 1.7 Tmol C yr^{-1} is sequestered from the atmosphere [*Cooley et al.*, 2007; *Subramaniam et al.*, 2008], reversing the WTNA's expected role as a net carbon source of ~2.5 Tmol C yr^{-1} were the plume's effects to be excluded [*Takahashi et al.*, 2002; *Mikaloff-Fletcher et al.*, 2007].

[3] A key hypothesis put forth by *Subramaniam et al.* [2008] is that diatom-diazotroph associations (DDAs) drive an efficient biological pump in tropical river plumes. On or near the continental shelf, N derived from inland sources is rapidly consumed, leaving a large area (~10^6 km^2) of lower-salinity, iron-rich surface waters in the WTNA that has excess dissolved Si and P relative to Redfield-Brzezinski stoichiometry (vs. C:Si:N:P = 106:15:16:1) [*Brzezinski*, 1985; *Shipe et al.*, 2007; *Subramaniam et al.*, 2008]. This N-depleted region in the outer plume (30 < Salinity (S) < 35) may be an ecological niche for diazotrophs and their diatom symbionts. The diazotroph *Richelia intracellularis* fixes N_2 to support its diatom hosts *Hemiaulus* spp. or *Rhizosolenia* spp. [*Foster et al.*, 2011], which may drive carbon sequestration in this region [*Carpenter et al.*, 1999; *Foster et al.*, 2007; *Subramaniam et al.*, 2008]. A quantitative link between the ecology, primary production, and carbon export in the *Hemiaulus*-dominated region has not yet been established, however, due to variations in geochemical, biological, and physical processes occurring on timescales from hours to weeks. Instantaneous measurements of primary productivity and export rarely represent time-averaged areal productivity, and geochemical tracers integrate biogeochemical cycling over a range of time periods. Here, we report the results of a primary productivity study using dissolved O_2 and DIC, which integrate the surface ecosystem productivity signal on timescales ranging from several days to one month [*Bender and Grande*, 1987; *Emerson*, 1987; *Luz and Barkan*, 2000; *Cooley and Yager*, 2006]. We confirm the efficient export of carbon during DDA blooms in the outer Amazon plume.

2. Methods

[4] Carbon and nutrient cycling and ecology of the Amazon plume's mixed layer was studied during the period of maximum river discharge in 2010 (May-June) onboard the *R/V Knorr*. During this time, the plume is carried North-West

[1]Department of Earth and Space Sciences, University of California, Los Angeles, California, USA.
[2]Department of Earth Sciences, University of Southern California, Los Angeles, California, USA.
[3]Horn Point Laboratory, Center for Environmental Science, University of Maryland, Cambridge, Maryland, USA.
[4]School of Biology, Georgia Institute of Technology, Atlanta, Georgia, USA.
[5]Romberg Tiburon Center and Department of Biology, San Francisco State University, Tiburon, California, USA.
[6]Virginia Institute of Marine Science, Gloucester Point, Virginia, USA.
[7]Max Planck Institute for Marine Microbiology, Bremen, Germany.
[8]Department of Biological Sciences and Wrigley Institute for Environmental Studies, University of Southern California, Los Angeles, California, USA.
[9]Department of Marine Sciences, University of Georgia, Athens, Georgia, USA.

Corresponding author: L. Y. Yeung, Department of Earth and Space Sciences, University of California, Los Angeles, CA 90095, USA. (lyyeung@ucla.edu)

0094-8276/12/2012GL053356

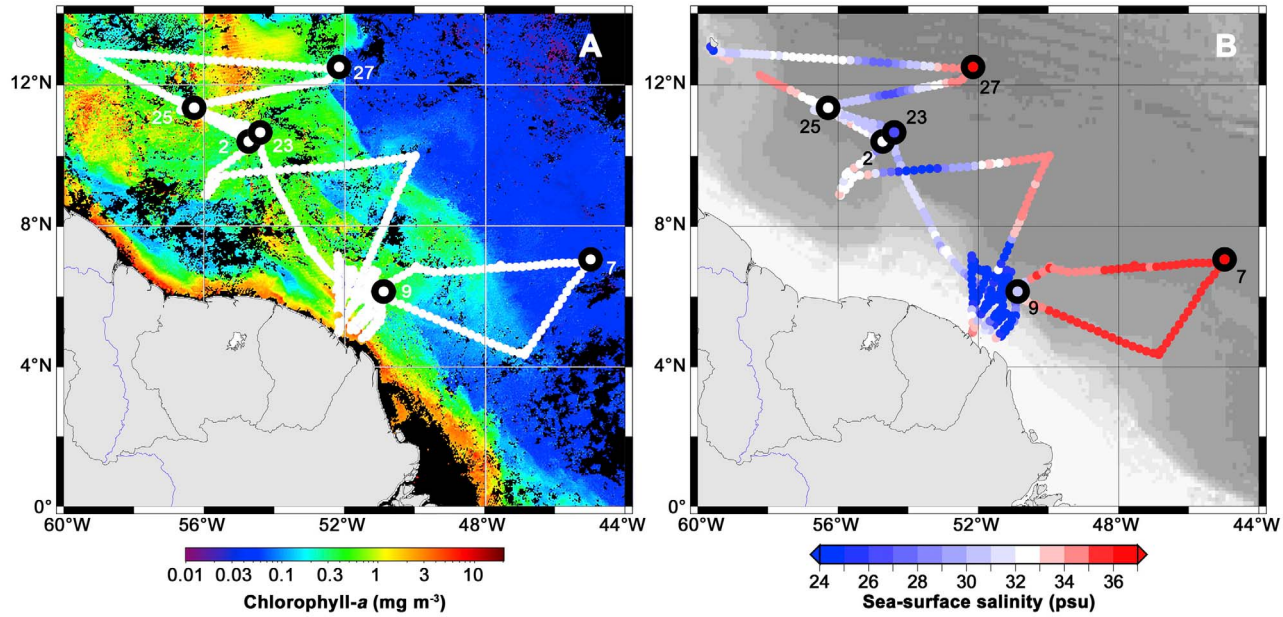

Figure 1. (a) Cruise track and sampling locations superimposed on the average sea surface chlorophyll-*a* concentration during 12–15 June 2010 (MODIS Aqua satellite; NASA). (b) Sea surface salinity measured while underway, with sea-floor bathymetry in gray.

from the river mouth by the North Brazil Current. It is characterized by a spatially variable enhancement in chlorophyll-*a* (Figure 1a) and a reduction in sea surface salinity (Figure 1b) in the WTNA.

[5] We report net-community and gross productivity at six cruise stations (12.5°N/45.0°E – 4.3°N/56.8°E; $26 < S < 36$). At each station, multiple casts of the CTD-rosette system were used to obtain depth profiles for key variables. Mixed-layer depths, which ranged from 5 – 40 m at these stations (Table 1), were determined as the depth at which the potential density (σ_θ) had decreased by 0.2 from the value at 2 m. We typically sampled 2 – 4 depths in the mixed layer and 6 – 8 depths within the upper 100 m.

[6] DDAs and *Synechococcus* spp. were enumerated by gravity-filtering cells from a 10-L Niskin bottle onto Nuclepore filters and counting transects under green excitation (see auxiliary material).[1] Phytoplankton counts were depth-integrated and an average count per liter for the mixed layer is reported except at Station 9, where only the surface value is reported. The average DDA abundance in the mixed layer was typically consistent with the abundance at the surface within ~25%.

[7] Seawater samples for oxygen triple isotopes ($^{17}\Delta$), O_2/Ar, DIC, dissolved Si, and water-$\delta^{18}O$ analyses were obtained from Niskin bottles at 2 – 4 depths in the mixed layer and at least one depth just below the pycnocline. DIC samples (500 mL) were collected and preserved according to standard protocols, and analyzed at the University of Georgia (precision < 1 umol kg^{-1} [*Cooley and Yager*, 2006]). Seawater for simultaneous O_2/Ar and $^{17}\Delta$ analysis (~270 mL) was siphoned into pre-evacuated (<1 mTorr) and pre-poisoned (100 μL saturated $HgCl_2$ solution) 500-mL flasks equipped with a vacuum valve [*Emerson et al.*, 1999]. Dissolved O_2 and Ar were analyzed at UCLA using an isotope ratio mass spectrometer (see auxiliary material). Silicate samples were run at sea using a LaChat autoanalyzer

[1]Auxiliary materials are available in the HTML. doi:10.1029/2012GL053356.

Table 1. Mixed-Layer Chemical and Biological Inventories and *In Situ* Productivities at Each Station[a]

Waters	Salinity[b]	Date	Station	Mixed-layer Depth (m)	Plume Thickness (m)	DDA counts (L^{-1})	Si (μM)	ΔDIC_{BIO} (mmol C m^{-2})	NOP (mmol O_2 m^{-2} d^{-1})	GOP (mmol O_2 m^{-2} d^{-1})	NOP/GOP[d]
Low-Salinity	26.5	6/17/10	23	9	9	1,927	25.1	32 ± 6	−4.8 ± 0.2	101 ± 43	−0.06 ± 0.02
	27.2[b]	6/4/10	9	5	5	161	21.4	nd[c]	13.3 ± 0.9	101 ± 1	0.13 ± 0.01
Outer plume	31.9	6/18/10	25	14	20	259,838	2.8	774 ± 16	84.5 ± 2.1	245 ± 21	0.35 ± 0.02
	32.1[b]	5/24/10	2	17	21	416,806	5.1	495 ± 13	72.4 ± 1.3	167 ± 29	0.47 ± 0.07
Oceanic	35.9	5/31/10	7	37	-	38	0.8	308 ± 58	10.6 ± 2.3	134 ± 46	0.09 ± 0.01
	36.0	6/21/10	27	19	-	128	1.2	156 ± 24	19.2 ± 0.9	169 ± 14	0.12 ± 0.01

[a]Uncertainties reflect ±1 s.e. of replicates. Gas-exchange uncertainties for NOP and GOP are likely ±20% for the wind speeds observed in this study (2–11 m s^{-1}) [*Ho et al.*, 2011]. Shipboard 24-h wind averages agreed with satellite wind-field averages within 0.5 m s^{-1} (RMSD). See the auxiliary material for data from individual replicates.

[b]Salinities correspond to Niskin bottle values for Si/DIC samples. These values were identical to those for diatom and O_2 samples except at Stations 9 and 2, where $S = 29.6$ and 33.1, respectively, for diatom samples, and $S = 30.4$ and 32.8, respectively, for O_2 samples (see Figure 2).

[c]Profiles for DIC taken on CTD casts with significantly different surface salinities (i.e., $S = 32.7$ at Station 9).

[d]NOP/GOP is insensitive to gas exchange uncertainties; NOP/GOP values reflect average of replicates, not the mean NOP and GOP values in this table.

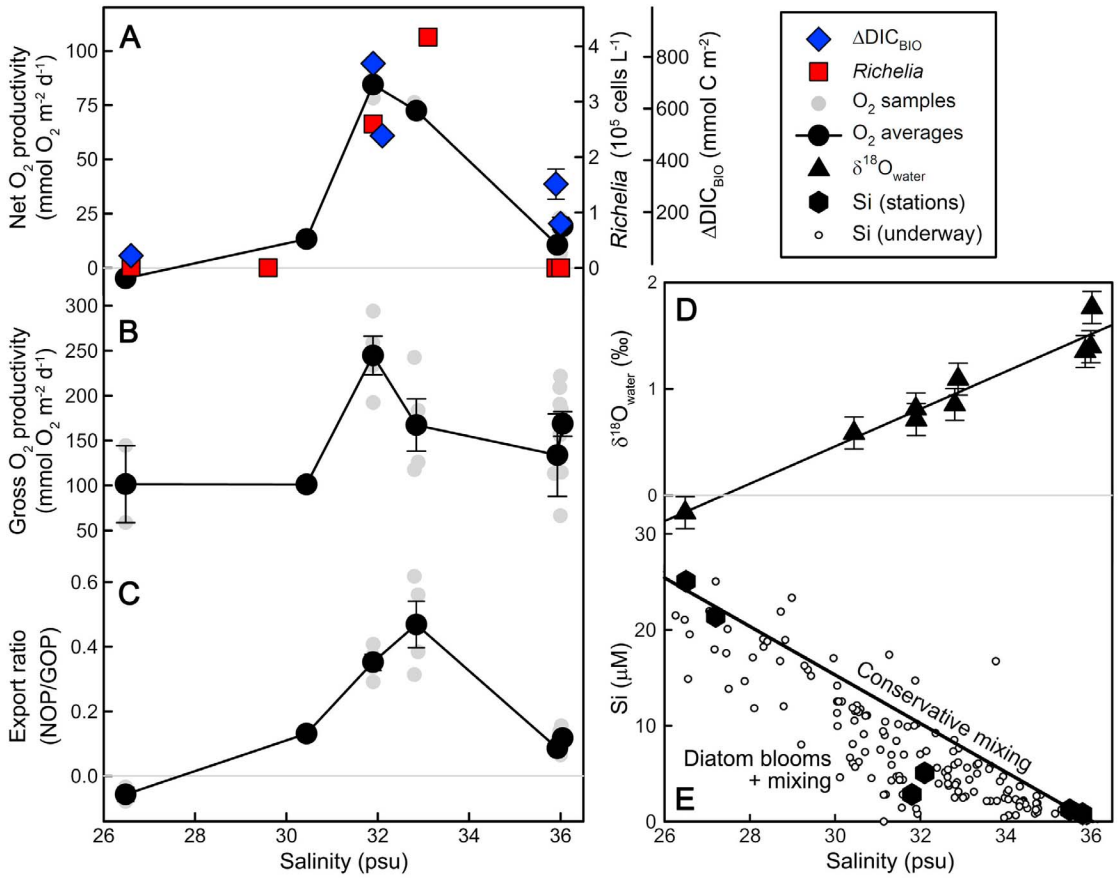

Figure 2. Effect of DDA blooms on dissolved chemical budgets, using salinity as a conserved tracer of physical mixing. (a) *R. intracellularis-H. hauckii* DDA abundance, NOP, and ΔDIC_{BIO}, which are all elevated in DDA blooms; (b) GOP, which is relatively invariant; (c) ecosystem export ratio (NOP/GOP), which is elevated more than twofold in blooms; (d) $\delta^{18}O$ of mixed-layer water, which reflects two-endmember mixing between the WTNA and the Amazon river. The regression line shown implies that $\delta^{18}O = -4.8‰$ at $S = 0$, whereas $\delta^{18}O$ of Amazon River water has $\delta^{18}O \sim -5‰$ [*Richey et al.*, 1989]; (e) Si, whose major non-mixing deficits probably reflect diatom blooms. Error bars reflect 1 s.e. except in Figure 2d, where they are 1 s.d. of each analysis.

(QuickChem 8000) and standard colorimetric protocols [*Strickland and Parsons*, 1972].

[8] We used several productivity proxies: the $^{17}\Delta$ method for gross O_2 productivity (GOP) [*Luz and Barkan*, 2000; *Prokopenko et al.*, 2011], O_2/Ar ratios for net O_2 productivity (NOP) [*Emerson*, 1987; *Hamme et al.*, 2012], and biological DIC drawdown for net community production (ΔDIC_{BIO}) [*Cooley and Yager*, 2006]. Gross O_2 productivity was calculated from $^{17}\Delta$ data using the method of *Prokopenko et al.* [2011]. Gas-exchange velocities, calculated from ASCAT wind histories of the 30 days prior to sample collection [*Ho et al.*, 2006; *Reuer et al.*, 2007], yielded O_2 residence times of 3 – 9 days in the mixed layer. Mixing through the surface halocline was calculated to be negligible (see auxiliary material). The estimated DIC residence time in the mixed layer is 22 – 30 days [*Cooley and Yager*, 2006], but it is poorly constrained because it depends on the kinetics of the carbonate system, the air-sea exchange rate, and the mixed-layer depth.

[9] Productivity is presented along the plume salinity gradient because salinity is a conserved tracer for river-ocean mixing [*Salisbury et al.*, 2011]; this assertion was validated against the $\delta^{18}O$ of H_2O, performed at the UC-Davis Stable Isotope Facility using laser spectrometry (see Figure 2). Mixed-layer salinity also reflects the extent of river influence on the surface ocean community [*Subramaniam et al.*, 2008].

3. Results and Discussion

[10] Phytoplankton communities varied along the salinity gradient, and net community productivity co-varied, in particular, with the abundance of *Richelia* heterocysts that were associated with *Hemiaulus hauckii* (1 – 2 heterocysts per diatom frustrule; Figure 2a and Table 1). Net O_2 productivity ranged from slightly heterotrophic at Station 23 (-4.8 mmol O_2 m^{-2} d^{-1}; $S = 26.5$) to highly autotrophic at Stations 2 and 25 in the outer plume (72.4 and 84.5 mmol O_2 m^{-2} d^{-1}, respectively; $S = 32 – 33$). Depth-integrated ΔDIC_{BIO} also co-varied with NOP, ranging from 32 to 774 mmol C m^{-2}. At outer-plume stations, NOP increased fivefold, and ΔDIC_{BIO} increased threefold, relative to their average values at high-salinity ($S = 36$) oceanic stations. These increases coincided with a high abundance of *H. hauckii-R. intracellularis* DDAs, which varied a thousand-fold between outer-plume stations and oceanic stations. The abundance of

Synechococcus and other phytoplankton, in contrast, did not vary with net community productivity (see auxiliary material). We therefore refer to the outer-plume stations, characterized by high DDA abundance, NOP, and ΔDIC_{BIO}, as DDA bloom stations.

[11] The fraction of primary production available for export from the surface layer is represented by the NOP/GOP ratio [*Bender*, 2000]. This ratio constrains the mechanism behind increased net community productivity in DDA blooms by distinguishing between increases in gross productivity versus the export ratio. Comparing NOP/GOP ratios with GOP (Figures 2b and 2c and Table 1), we find that the high NOP at DDA bloom stations is due mainly to an increased export ratio. GOP varied less than NOP, averaging 134 ± 33 mmol O_2 m^{-2} d^{-1} (1σ s.d.) across all stations except bloom Station 25, where it was 245 ± 21 mmol O_2 m^{-2} d^{-1} (1 s.e., n = 4). Resulting community export ratios were ~0.1 for oceanic stations and ~0.4 in the DDA blooms, which is a value approaching the physiological upper limit [*Halsey et al.*, 2010]. These export ratios are 3 – 4 times higher than those presumed for the Amazon plume in previous studies [*Carpenter et al.*, 1999; *Cooley and Yager*, 2006; *Cooley et al.*, 2007]. Similar export ratios were observed for diatoms during a bloom in the Bering Sea [*Prokopenko et al.*, 2011] and in N-depleted mesocosm experiments [*Engel et al.*, 2002]; they likely reflect spatio-temporal decoupling of primary production and upper-ocean heterotrophy on timescales of days to a week [*Riemann et al.*, 2000; *Yager et al.*, 2001].

[12] Quantitative comparison of these short-term NOP results with ΔDIC_{BIO} offers further insight to relevant time scales and impacts of DDA blooms on the longer-term DIC budget in the WTNA. Our measured ΔDIC_{BIO} at oceanic stations ranged from 156 – 308 mmol C m^{-2}. Thus, the implied mean net community productivity over a 30-day residence time for DIC in this region [*Cooley and Yager*, 2006] ranges from 5 – 14 mmol C m^{-2} d^{-1}. This range is similar to the range of NOP-based net community productivity at oceanic stations (12.4 – 14.9 mmol C m^{-2} d^{-1}) calculated using the average NOP at Stations 7 and 27 (14.9 mmol O_2 m^{-2} d^{-1}) and a photosynthetic quotient of 1 – 1.2 for growth supported by N_2 fixation [*Cox*, 1966; *Stal and Walsby*, 1998]. High-salinity waters on the edges of the plume, which are only slightly undersaturated in DIC, nonetheless appear to be net autotrophic [*Cooley and Yager*, 2006; *Cooley et al.*, 2007].

[13] Accounting for the large ΔDIC_{BIO} at DDA bloom stations (495 – 774 mmol C m^{-2}) requires an average net community productivity of 16.5 – 25.8 mmol C m^{-2} d^{-1} over ~30 days [*Hu et al.*, 2004]. Some periods of high productivity in excess of that at oceanic or low-salinity stations (3.5 – 4.3 mmol C m^{-2}, derived from the average NOP at Stations 9 and 23) are therefore required. At a rate of 1 division day^{-1} observed in the field for *H. hauckii* communities in oligotrophic waters [*Furnas*, 1991], the thousand-fold DDA population increase at DDA bloom stations relative to oceanic populations would occur in ten days. Similarly, about 7 – 10 days of bloom-like net community productivity (65.4 – 78.5 mmol C m^{-2} d^{-1}) during a 30-day interval can explain the ΔDIC_{BIO} values at DDA bloom stations.

[14] Nearly all of the measured ΔDIC_{BIO} at DDA bloom stations could be attributed to net community productivity supported by diazotrophy in DDA blooms. However, coastal diatoms growing on river-borne nitrate could also contribute to the measured ΔDIC_{BIO}. A bloom of coastal diatoms dominated by, e.g., *Pseudo-nitzschia* spp. and *Skeletonoma costatum* (10^6 cells L^{-1}) was indeed observed on the cruise (S = 22 – 23), and the net community production therein was high: ΔDIC_{BIO} ≈ 1400 mmol C m^{-2} and NOP ≈ 140 mmol O_2 m^{-2} d^{-1}, enough to exhaust the riverine nitrate supply of 12 – 23 μmol N L^{-1} [*DeMaster and Pope*, 1996]. Our NOP measurements, however, place a lower limit on the DIC drawdown by DDAs because the short mixed-layer residence time of O_2 renders O_2-based methods insensitive to productivity more than ~5 days prior to sampling at the DDA bloom stations. In 5 days, we calculate that DDAs alone account for 73% of ΔDIC_{BIO} at Station 2 (362 mmol C m^{-2}) and 55% of ΔDIC_{BIO} at Station 25 (423 mmol C m^{-2}).

[15] The dissolved Si budget of plume waters is also consistent with diatoms playing the primary role in the observed carbon drawdown. Silicate deficits, relative to conservative mixing of fresher, high-Si plume waters and salty, low-Si TNA waters, were observed in the areas of highest DDA abundance (Figure 2e and Table 1). We interpret these deficits as biological uptake during diatom growth between 26 < S < 36. Diatom blooms should consume Si at rates significantly faster than that of plume-ocean mixing (days vs. a month), so departures from the ideal mixing line allow one to estimate the biological uptake of Si. The Si vs. salinity river-ocean mixing line was calculated by using the mean Si concentration in the freshwater plume at low-salinity stations, and in the mixed layer at oceanic stations, as mixing endmembers (see Table 1). Si inventories were obtained by integrating Si depth profiles. We use the depth of the freshwater plume rather than the σ_θ -defined mixed-layer depth at plume stations because conservative mixing preserves Si and salt inventories in the low-salinity layer.

[16] From the Si deficits at stations 2 and 25, carbon uptake inventories of 440 and 750 mmol C m^{-2}, respectively, were calculated using a C:Si ratio of 4.5 for *H. hauckii* (presumed to be similar to that for *H. sinensis* [*Brzezinski*, 1985] because of similar morphology). These proxy-derived carbon uptake values are in remarkable agreement with ΔDIC_{BIO} at those stations (495 and 774 mmol C m^{-2}). While this analysis does not distinguish between DDAs and coastal diatoms, the Si uptake calculated here is expected to be supported primarily by diazotrophy. Coastal diatoms can exhaust the riverine nitrate supply before plume waters reach the salinity range of the Si uptake calculation (e.g., S = 22 vs. 26 < S < 36). Therefore, calculated Si uptake values likely represent Si uptake in regions where surface nitrate concentrations are negligible. There is some uncertainty in the mixing endmembers used in this analysis due to natural variability and limited spatial coverage, so the near-quantitative agreement between dissolved Si and ΔDIC_{BIO} could be serendipitous; more measurements are needed to validate this comparison. Underway Si measurements rarely achieve the full mixing-line value in this region, suggesting that diatom-driven, diazotroph-supported biological uptake of Si was widespread (see Figure 2) [*DeMaster and Pope*, 1996; *DeMaster et al.*, 1996; *Shipe et al.*, 2006]. These data, taken together with the GOP, NOP, and ΔDIC_{BIO} data, support a coupling between DDA biomass growth, carbon and silica drawdown, and export efficiency.

[17] The ^{15}N composition of organic matter in collected in sediment traps at 150 m suggests that at least some of this DDA-driven surface export reaches deeper waters. Organic matter containing recently fixed nitrogen has $\delta^{15}N = -1‰$, whereas deep-water nitrate and riverine nitrate have higher $\delta^{15}N \approx +5‰$ [*Karl et al.*, 1997; *Sigman et al.*, 2000; *Aufdenkampe et al.*, 2007]. Therefore, export of particulate organic carbon supported by recent N_2 fixation yields low $\delta^{15}N$ values in sediment-trap organic matter. At Stations 25 and 27, the particulate organic matter collected had $\delta^{15}N$ = 2.9‰ and 2.7‰, respectively; *Hemiaulus* frustrules and *Trichodesmium* trichomes were identified in those traps. In contrast, sediment traps at lower-salinity stations had higher $\delta^{15}N$ values (4.3‰ and 4.8‰ at stations 9 and 23, respectively) and no evidence for DDAs or other diazotrophs. While these $\delta^{15}N$ measurements do not distinguish between diazotrophs, the predominance of *Hemiaulus-Richelia* DDAs in the outer Amazon plume suggests that N_2 fixation by *Richelia* plays an important role in carbon export (see estimate in the auxiliary material).

[18] DDA blooms have also been found in other tropical river systems [*Zeev et al.*, 2008; *Foster et al.*, 2009; *Grosse et al.*, 2010], yet the factors controlling their development in freshwater plumes are not well understood. Estimates of total carbon export by DDAs are therefore poorly constrained. Satellite-based detection of DDA blooms is difficult because they do not always increase surface chlorophyll above typical threshold values [*Villareal et al.*, 2011]. Localized upwelling due to anticyclonic mesoscale eddies could play a role in DDA bloom formation [*Martin and Richards*, 2001; *Hu et al.*, 2004], so physical and biogeochemical modeling efforts incorporating DDAs are also needed. As drivers of N_2 fixation and carbon drawdown in river plumes and oligotrophic waters [*Karl et al.*, 2012; *Villareal et al.*, 2011], DDAs likely have a global impact that is sensitive to both climatic and anthropogenic influences.

[19] **Acknowledgments.** This work was supported by grants from the National Science Foundation (0929015, 0933975, 0934025, 0934035, 0934036, 934073, 0934095, 0961221, and 1049665) and the Gordon and Betty Moore Foundation. We thank L. S. Chong, J. Fleming, and K. Ziegler for shipboard and experimental assistance, the UC-Davis Stable Isotope Facility for water isotope analysis, and the captain and crew of the *R/V Knorr*. Discussions with A. Subramaniam and E. A Schauble, and comments from two anonymous reviewers, helped improve the paper.

[20] The Editor thanks two anonymous reviewers for assisting in the evaluation of this paper.

References

Aufdenkampe, A. K., E. Mayorga, J. I. Hedges, C. Llerena, P. D. Quay, J. Gudeman, A. V. Krusche, and J. E. Richey (2007), Organic matter in the Peruvian headwaters of the Amazon: Compositional evolution from the Andes to the lowland Amazon mainstem, *Org. Geochem.*, *38*, 337–364, doi:10.1016/j.orggeochem.2006.06.003.

Bender, M. L. (2000), Tracer from the sky, *Science*, *288*(5473), 1977–1978, doi:10.1126/science.288.5473.1977.

Bender, M. L., and K. D. Grande (1987), Production, respiration, and the isotope geochemistry of O_2 in the upper water column, *Global Biogeochem. Cycles*, *1*(1), 49–59, doi:10.1029/GB001i001p00049.

Brzezinski, M. A. (1985), The Si:C:N ratio of marine diatoms: Interspecific variability and the effect of some environmental variables, *J. Phycol.*, *21*(3), 347–357, doi:10.1111/j.0022-3646.1985.00347.x.

Carpenter, E. J., J. P. Montoya, J. Burns, M. R. Mulholland, A. Subramaniam, and D. G. Capone (1999), Extensive bloom of a N_2-fixing diatom/cyanobacterial association in the tropical Atlantic Ocean, *Mar. Ecol. Prog. Ser.*, *185*, 273–283, doi:10.3354/meps185273.

Cooley, S. R., and P. L. Yager (2006), Physical and biological contributions to the western tropical North Atlantic Ocean carbon sink formed by the Amazon River plume, *J. Geophys. Res.*, *111*, C08018, doi:10.1029/2005JC002954.

Cooley, S. R., V. J. Coles, A. Subramaniam, and P. L. Yager (2007), Seasonal variations in the Amazon plume-related atmospheric carbon sink, *Global Biogeochem. Cycles*, *21*, GB3014, doi:10.1029/2006GB002831.

Cox, R. M. (1966), Physiological studies on nitrogen fixation in the blue-green alga Anabaena cylindrica, *Arch. Mikrobiol.*, *53*, 263–276, doi:10.1007/BF00446673.

DeMaster, D. J., and R. H. Pope (1996), Nutrient dynamics in Amazon shelf waters: Results from AMASSEDS, *Cont. Shelf Res.*, *16*(3), 263–289, doi:10.1016/0278-4343(95)00008-O.

DeMaster, D. J., W. O. Smith Jr., D. M. Nelson, and J. Y. Aller (1996), Biogeochemical processes in Amazon shelf waters: Chemical distributions and uptake rates of silicon, carbon, and nitrogen, *Cont. Shelf Res.*, *16*(5–6), 617–643, doi:10.1016/0278-4343(95)00048-8.

Emerson, S. (1987), Seasonal oxygen cycles and biological new production in surface waters of the subarctic pacific ocean, *J. Geophys. Res.*, *92*(C6), 6535–6544, doi:10.1029/JC092iC06p06535.

Emerson, S., C. Stump, D. Wilbur, and P. Quay (1999), Accurate measurement of O_2, N_2, and Ar gases in water and the solubility of N_2, *Mar. Chem.*, *64*(4), 337–347, doi:10.1016/S0304-4203(98)00090-5.

Engel, A., S. Goldthwait, U. Passow, and A. Alldredge (2002), Temporal decoupling of carbon and nitrogen dynamics in a mesocosm diatom bloom, *Limnol. Oceanogr.*, *47*(3), 753–761, doi:10.4319/lo.2002.47.3.0753.

Foster, R. A., A. Subramaniam, C. Mahaffey, E. J. Carpenter, D. G. Capone, and J. P. Zehr (2007), Influence of the Amazon River plume on distributions of free-living and symbiotic cyanobacteria in the western tropical north Atlantic Ocean, *Limnol. Oceanogr.*, *52*(2), 517–532, doi:10.4319/lo.2007.52.2.0517.

Foster, R. A., A. Subramaniam, and J. P. Zehr (2009), Distribution and activity of diazotrophs in the eastern equatorial Atlantic, *Environ. Microbiol.*, *11*(4), 741–750, doi:10.1111/j.1462-2920.2008.01796.x.

Foster, R. A., M. M. M. Kuypers, T. Vagner, R. W. Paerl, N. Musat, and J. P. Zehr (2011), Nitrogen fixation and transfer in open ocean diatom-cyanobacterial symbioses, *ISME J.*, *5*, 1484–1493, doi:10.1038/ismej.2011.26.

Furnas, M. J. (1991), Net in situ growth rates of phytoplankton in an oligotrophic, tropical shelf ecosystem, *Limnol. Oceanogr.*, *36*(1), 13–29, doi:10.4319/lo.1991.36.1.0013.

Grosse, J., D. Bombar, H. N. Doan, L. N. Nguyen, and M. Voss (2010), The Mekong River plume fuels nitrogen fixation and determines phytoplankton series distribution in the South China Sea during low- and high-discharge season, *Limnol. Oceanogr.*, *55*(4), 1668–1680, doi:10.4319/lo.2010.55.4.1668.

Halsey, K. H., A. J. Milligan, and M. J. Behrenfeld (2010), Physiological optimization underlies growth rate-independent chlorophyll-specific gross and net primary production, *Photosynth. Res.*, *103*, 125–137, doi:10.1007/s11120-009-9526-z.

Hamme, R. C., et al. (2012), Dissolved O_2/Ar and other methods reveal rapid changes in productivity during a Lagrangian experiment in the Southern Ocean, *J. Geophys. Res.*, *117*, C00F12, doi:10.1029/2011JC007046.

Ho, D. T., C. S. Law, M. J. Smith, P. Schlosser, M. Harvey, and P. Hill (2006), Measurements of air-sea gas exchange at high wind speeds in the Southern Ocean: Implications for global parameterizations, *Geophys. Res. Lett.*, *33*, L16611, doi:10.1029/2006GL026817.

Ho, D. T., R. Wanninkhof, P. Schlosser, D. S. Ullman, D. Hebert, and K. F. Sullivan (2011), Toward a universal relationship between wind speed and gas exchange: Gas transfer velocities measured with $^3He/SF_6$ during the Southern Ocean Gas Exchange Experiment, *J. Geophys. Res.*, *116*, C00F04, doi:10.1029/2010JC006854.

Hu, C. M., E. T. Montgomery, R. W. Schmitt, and F. E. Muller-Karger (2004), The dispersal of the Amazon and Orinoco River water in the tropical Atlantic and Carribean Sea: Observation from space and S-PALACE floats, *Deep Sea Res., Part II*, *51*(10–11), 1151–1171.

Karl, D., R. Letelier, L. Tupas, J. Dore, J. Christan, and D. Hebel (1997), The role of nitrogen fixation in biogeochemical cycling in the subtropical North Pacific Ocean, *Nature*, *388*, 533–538, doi:10.1038/41474.

Karl, D. M., M. J. Church, R. M. Letelier, and C. Mahaffey (2012), Predictable and efficient carbon sequestration in the North Pacific Ocean supported by symbiotic nitrogen fixation, *Proc. Natl. Acad. Sci. U. S. A.*, *109*(6), 1842–1849, doi:10.1073/pnas.1120312109.

Körtzinger, A. (2003), A significant CO_2 sink in the tropical Atlantic Ocean associated with the Amazon River plume, *Geophys. Res. Lett.*, *30*(24), 2287, doi:10.1029/2003GL018841.

Luz, B., and E. Barkan (2000), Assessment of oceanic productivity with the triple-isotope composition of dissolved oxygen, *Science*, *288*(5473), 2028–2031, doi:10.1126/science.288.5473.2028.

Martin, A. P., and K. P. Richards (2001), Mechanisms for vertical nutrient transport within a North Atlantic mesoscale eddy, *Deep Sea Res., Part II*, *48*(4–5), 757–773, doi:10.1016/S0967-0645(00)00096-5.

Mikaloff-Fletcher, S. E., et al. (2007), Inverse estimates of the oceanic sources and sinks of natural CO_2 and implied oceanic carbon transport, *Global Biogeochem. Cycles*, *21*, GB1010, doi:10.1029/2006GB002751.

Prokopenko, M. G., O. M. Pauluis, J. Granger, and L. Y. Yeung (2011), Exact evaluation of gross photosynthetic production from the oxygen triple-isotope composition of O_2: Implications for the net-to-gross primary production ratios, *Geophys. Res. Lett.*, *38*, L14603, doi:10.1029/2011GL047652.

Reuer, M. K., B. A. Barnett, M. L. Bender, P. G. Falkowski, and M. B. Hendricks (2007), New estimates of Southern Ocean biological production rates from O_2/Ar ratios and the triple isotope composition of O_2, *Deep Sea Res., Part I*, *54*(6), 951–974, doi:10.1016/j.dsr.2007.02.007.

Richey, J. E., L. A. K. Mertes, T. Dunne, R. L. Victoria, B. R. Forsberg, A. C. N. S. Tancredi, and E. Oliveira (1989), Sources and routing of the Amazon River flood wave, *Global Biogeochem. Cycles*, *3*(3), 191–204, doi:10.1029/GB003i003p00191.

Riemann, L., G. F. Steward, and F. Azam (2000), Dynamics of bacterial community composition and activity during a mesocosm diatom bloom, *Appl. Environ. Microbiol.*, *66*(2), 578–587, doi:10.1128/AEM.66.2.578-587.2000.

Salisbury, J., D. Vandemark, J. Campbell, C. Hunt, D. Wisser, N. Reul, and B. Chapron (2011), Spatial and temporal coherence between Amazon River discharge, salinity, and light absorption by colored organic carbon in western tropical Atlantic surface waters, *J. Geophys. Res.*, *116*, C00H02, doi:10.1029/2011JC006989.

Shipe, R. F., J. Curtaz, A. Subramaniam, E. J. Carpenter, and D. G. Capone (2006), Diatom biomass and productivity in oceanic and plume-influenced waters of the western tropical Atlantic Ocean, *Deep Sea Res., Part I*, *53*, 1320–1334, doi:10.1016/j.dsr.2006.05.013.

Shipe, R. F., E. J. Carpenter, S. R. Govil, and D. G. Capone (2007), Limitation of phytoplankton production by Si and N in the western Atlantic Ocean, *Mar. Ecol. Prog. Ser.*, *338*, 33–45, doi:10.3354/meps338033.

Sigman, D. M., M. A. Altabet, D. C. McCorkle, R. François, and G. Fischer (2000), The δ^{15}N of nitrate in the Southern Ocean: Nitrogen cycling and circulation in the ocean interior, *J. Geophys. Res.*, *105*(C8), 19,599–19,614, doi:10.1029/2000JC000265.

Stal, L. J., and A. E. Walsby (1998), The daily integral of nitrogen fixation by planktonic cyanobacteria in the Baltic Sea, *New Phytol.*, *139*, 665–671, doi:10.1046/j.1469-8137.1998.00228.x.

Strickland, J. D. H., and T. R. Parsons (1972), *A Practical Handbook of Seawater Analysis*, 2nd ed., Fish. Res. Board of Can., Ottawa.

Subramaniam, A., et al. (2008), Amazon River enhances diazotrophy and carbon sequestration in the tropical North Atlantic Ocean, *Proc. Natl. Acad. Sci. U. S. A.*, *105*(30), 10,460–10,465, doi:10.1073/pnas.0710279105.

Takahashi, T., et al. (2002), Global sea-air CO_2 flux based on climatological surface ocean pCO_2, and seasonal, biological and temperature effects, *Deep Sea Res., Part II*, *49*(9–10), 1601–1622, doi:10.1016/S0967-0645(02)00003-6.

Ternon, J. F., C. Oudot, A. Dessier, and D. Diverres (2000), A seasonal tropical sink for atmospheric CO_2 in the Atlantic Ocean: The role of the Amazon River discharge, *Mar. Chem.*, *68*(3), 183–201, doi:10.1016/S0304-4203(99)00077-8.

Villareal, T. A., L. Adornato, C. Wilson, and C. A. Schoenbaechler (2011), Summer blooms of diatom-diazotroph assemblages and surface chlorophyll in the North Pacific gyre: A disconnect, *J. Geophys. Res.*, *116*, C03001, doi:10.1029/2010JC006268.

Yager, P. L., T. L. Connelly, B. Mortazavi, K. E. Wommack, N. Bano, J. E. Bauer, S. Opsahl, and J. T. Hollibaugh (2001), Dynamic bacterial and viral response to an algal bloom at subzero temperatures, *Limnol. Oceanogr.*, *46*(4), 790–801, doi:10.4319/lo.2001.46.4.0790.

Zeev, E. B., T. Yogev, D. Man-Aharonovich, N. Kress, B. Herut, O. Béjà, and I. Berman-Frank (2008), Seasonal dynamics of the endosymbiotic, nitrogen-fixing cyanobacterium *Richelia intracellularis* in the eastern Mediterranean Sea, *ISME J.*, *2*(9), 911–923, doi:10.1038/ismej.2008.56.